Res Chem Intermed (2017) 43:245–257
DOI 10.1007/s11164-016-2618-4

Generation of sulfate radicals by supported ruthenium catalyst for phenol oxidation in water

Mansoor Anbia[1] · **Marzie Rezaie**[1]

Received: 12 February 2016 / Accepted: 20 June 2016 / Published online: 12 July 2016

Abstract In this study we report the preparation of $RuO_2/Fe_3O_4@nSiO_2@mSiO_2$ core–shell powder mesoporous catalyst for heterogeneous oxidation of phenol by peroxymonosulfate (PMS) as oxidant. The properties of this supported catalyst were characterized by SEM–EDS (scanning electron microscopy–energy dispersive X-ray spectroscopy), XRD (powder X-ray diffraction), TEM (transmission electron microscopy), and nitrogen adsorption–desorption. It is found that using ruthenium oxide-based catalyst is highly effective in activating PMS for related sulfate radicals. The effects of catalyst loading, phenol concentration, PMS concentration, reaction temperature, and reusability of the as-prepared catalyst on phenol degradation were investigated. In $RuO_2/Fe_3O_4@nSiO_2@mSiO_2$ mesoporous catalyst, Oxone (PMS) was effectively activated and 100 % phenol degradation occurred in 40 min. The magnetic $RuO_2/Fe_3O_4@nSiO_2@mSiO_2$ catalyst was facility separated from the solution by an external magnetic field. To regenerate the deactivated catalyst and improve its catalytic properties, three different methods involving annealing in air, washing with water, and applying ultrasonics were used. The catalyst was recovered thoroughly by heat treatment.

Keywords $RuO_2/Fe_3O_4@nSiO_2@mSiO_2$ mesoporous catalyst · Peroxymonosulfate (PMS) · Advanced oxidation processes (AOPs) · Phenol degradation · Magnetic separation

✉ Mansoor Anbia
anbia@iust.ac.ir

[1] Research Laboratory of Nanoporous Materials, Faculty of Chemistry, Iran University of Science and Technology, Farjam Street, Narmak, Tehran 16846-13114, Iran

Introduction

In recent years, most industrial processes produce large amounts of organic contaminants. The main water pollutants are phenol and its derivatives, which have toxic effects on the environment even at low concentrations [1–5]. Therefore, they must be eliminated before release in the natural environment.

The byproducts of several industries such as the chemical industries, petroleum refining, petrochemical industries, and pharmaceutical industries are phenolic contaminants [6, 7]. Among the feasible technologies for wastewater treatment, AOPs (advanced oxidation processes) using chemical compounds as oxidants have attracted much attention in water treatment owing to high conversion of organic pollutants [8–10].

In principle, the catalytic oxidation process is used to convert the toxic organic compounds into harmless products such as CO_2 and H_2O [11].

Homogenous catalytic oxidation using Fenton's reagent has demonstrated an effective ability to degrade toxic organics in aqueous solution [12–15]. However, these catalysts need long-term processes for their separation from the medium [16].

In addition, many homogenous catalysts are harmful to the environment, because they dissolve in water. To overcome this problem, heterogeneous catalysts that can be easily retrieved and reused are being applied [17, 18]. Furthermore, heterogeneous catalysts can easily mineralize organic compounds to undergo reactions. They can completely convert to CO_2 and H_2O or moderately oxidize the organic compounds to less toxic ones [9, 10].

The Fenton process is one of the most popular methods to degrade organic compounds in wastewater, which involves hydrogen peroxide and Fe ions (Fenton reagent) to create hydroxyl radicals in solutions [8, 15].

Nowadays, some other oxidants such as peroxymonosulfate have been proposed. The high oxidation potential of sulfate radicals has caused them to be suggested as an alternative recently [19]. For the oxidation of organic pollutants to harmless end products, conjunction of heavy metals such as cobalt and iron with PMS to produce sulfate radicals has been proposed. The radical generation process can be described as the following: [19].

$$Co^{2+} + HSO_5^- \rightarrow Co^{3+} + OH^- + SO_4^{\cdot -}, \quad (1)$$

$$Co^{3+} + HSO_5^- \rightarrow Co^{2+} + H^+ + SO_5^{\cdot -}. \quad (2)$$

The oxidation processes with heavy metals/PMS have higher degradation efficiency than the Fenton process. Moreover, the oxidation by sulfate radicals is less related to the pH of a solution, providing a good way to efficiently degrade organic contaminants [19, 20]. The main issue in the use of metal ions as catalysts is their toxicity causing health problems to humans. Therefore, utilization of heterogeneous catalysts (supported catalysts) has been proposed. Ruthenium is one of the popular transition metals that it can be used as a catalyst in the degradation of organic contaminants. This noble metal has been used traditionally as a heterogeneous catalyst for water treatment [21]. Oliviero et al. [22] used Ru as

catalyst in catalytic wet air oxidation of phenol and acrylic acid. They found that Ru was very reactive to phenol degradation. Similar studies in degradation of organic compounds by using ruthenium-based catalysts have been reported [16, 23–25]. These reports show that ruthenium had very good efficiency. However, the utilization of this heavy metal-based catalyst with PMS for phenol oxidation is less developed. This paper investigates the use of ruthenium heterogeneous catalyst with peroxymonosulfate for chemical mineralizing of phenol in aqueous solution. For the synthesis of supported catalysts, the metal ions should be loaded into solid supports. In the water treatment processes, mesoporous silica materials are the best option as an adsorbent and catalyst, due to their nontoxicity, high mechanical and chemical resistance, large pore volume, and high surface area [26].

Since the separation of the catalyst from solution, especially when the volume of the solution is high, is time-consuming, the use of superparamagnetic materials for catalytic applications has been developed [27]. These materials can easily be retrieved by a magnetic field and reused.

In this paper, we present a new synthesis of core–shell structured microsphere with a magnetic core, a middle nonporous silica shell, and an outer ruthenium-functionalized mesoporous silica shell ($RuO_2/Fe_3O_4@nSiO_2@mSiO_2$). This catalyst has shown high magnetic separation performance and activity in oxidation of phenol solutions.

Experimental

Chemicals

Deionized water was used to perform the experiments and prepare solutions. The chemical substances used in this paper were obtained from Sigma-Aldrich Company.

Preparation of Fe_3O_4

At first, 5 g $FeCl_3{\cdot}6H_2O$ and 2 g $FeCl_2{\cdot}4H_2O$ was dissolved in deionized water under permanent stirring. Then, 30 % (w/v) NaOH solution was added dropwise with nitrogen bubbling so that the pH of the solution reached 10 and magnetic Fe_3O_4 nanoparticles were synthesized. After constant stirring of the reaction mixture for 30 min, the vessel was transferred to an oil bath to be heated at 90 °C for 1 h. After that, the end black nanoparticles were cooled down to room temperature, and then they were washed with a mixture of ethanol/water for several times and dried at 60 °C overnight.

Preparation of $Fe_3O_4@nSiO_2@mSiO_2$

Fe_3O_4/silica spheres were synthesized by hydrolysis reaction. First, 2 g Fe_3O_4 was washed by HCl solution (0.1 M) and then transferred to a solution containing 1 mL of aqueous ammonia (25 wt%), 80 mL ethanol, and 20 mL H_2O. After dispersing

for 15 min, 1 mL tetraethyl orthosilicate (TEOS) was added dropwise into the reaction solution and stirred intensively at room temperature for 12 h. The obtained material was divided and washed with ethanol and deionized water and then dispersed in a solution containing 6 g CTAB, 80 mL deionized water, 60 mL ethanol, and 1.2 mL of aqueous ammonia (25 wt%) for 0.5 h. In the next step, 9 mL of TEOS was added to the above mixture under stirring. After reacting for 12 h, the product was separated with a magnet and washed with ethanol and deionized water. In the final step, surfactant template was removed by dispersing particles in 100 mL of ethanol and refluxed at 90 °C for 48 h. The final product was dried at 60 °C, and denoted as $Fe_3O_4@nSiO_2@mSiO_2$.

Preparation of $RuO_2/Fe_3O_4@nSiO_2@mSiO_2$ catalyst

A general impregnation method was used for the synthesis of $RuO_2/Fe_3O_4@nSiO_2@mSiO_2$ catalyst. At first, a fixed amount of $Fe_3O_4@nSiO_2@mSiO_2$ was dispersed in 90 mL of ethanol for 15 min, then ruthenium chloride (Sigma-Aldrich) and 50 mL ethanol were added to the solution and kept stirring vigorously for 16 h, and then dried at 60 °C. The resultant solid was heated at 200 °C for 2 h. The loading of Ru on the support was maintained at 10 wt%.

Characterization

The characterization of the obtained catalyst was performed by XRD (X-ray diffraction), SEM–EDS (scanning electron microscopy- energy dispersive X-ray spectroscopy), TEM (transmission electron microscopy), and N_2 adsorption–desorption.

The mineralogy and the structural features of the magnetic support and catalyst were studied by XRD (X-ray diffraction) patterns on a Bruker D8 Focus X-ray diffractometer with Cu-Kα ($\lambda = 0.154$) radiation at a current of 30 mA and voltage of 30 kV.

The morphological and textural information of the Fe_3O_4 cores were distinguished by using SEM (scanning electron microscopy) on a ZEISS NEON 40 EsB. EDS was also used to illustrate the ruthenium particles on the support.

The structures of particles were characterized by TEM (transmission electron microscopy) operated at 100 kV (Zeiss-EM10C).

The catalyst was also characterized by N_2 adsorption–desorption to identify the specific surface area. The support and catalyst were degassed at 120 °C for 12 h prior to the analysis.

Experimental procedure

To perform the catalytic oxidative examinations, 50 mL of phenol solution with initial concentration of 50 mg/L was poured into a 100 mL glass beaker and stirred constantly to obtain a homogeneous mixture at 25 °C, while the pH of the solution was adjusted to $\sim$7.0. Next, a certain amount of catalyst was added to the mixture and then it was allowed to reach adsorption equilibrium between phenol molecules and the catalyst during reaction time. The next step of the experiment was to blend an amount of Oxone as an active component and at the end of the reaction, an

excess content of sodium nitrite as a quenching reagent was added to the sample solutions. After catalytic oxidation experiments to determine the concentration of phenol, the magnetic catalyst was separated from the reaction medium by means of a magnet at a predetermined period of time and the spectrophotometric measurements were done using a standard method employing 4-aminoantipyrine at the maximum wavelength of phenol, i.e., 500 nm.

Results and discussion

Characterization of ruthenium impregnated Fe_3O_4@nSiO_2@mSiO_2 catalyst

XRD patterns of support and RuO_2/Fe_3O_4@nSiO_2@mSiO_2 are presented in Fig. 1. The core–shell materials exhibit diffraction patterns similar to that of Fe_3O_4 microspheres [28], suggesting that the silica shells were well-formed on the magnetic microspheres. Due to the amorphous nature of SiO_2, we cannot see a sharp peak in XRD pattern of Fe_3O_4@nSiO_2@mSiO_2 and, as can be observed in Fig. 1b, a broad peak around 2θ 20 is present in the patterns of as-prepared core/shell structure, and is associated with the SiO_2 layer. It can be seen that ruthenium species are found in the form of RuO_2 on RuO_2/Fe_3O_4@nSiO_2@mSiO_2 in Fig. 1c.

Morphology and structural properties of the synthesized Fe_3O_4 nanoparticles were investigated by SEM images. Figure 2a shows the sphere-like morphology of Fe_3O_4 core nanoparticles, the particle size varied between 20 and 50 nm. The EDS measurement displays the presence of elements, C, O, Fe, Si, and Ru. Thus, the EDS spectra confirm the XRD results. This analysis was carried out before and after reaction to investigate the Ru wt%. After reaction, the Ru was about 8 wt%. The results are shown in Fig. 2b, c.

TEM images of particles show the core/shell structure of Fe_3O_4@nSiO_2@mSiO_2 as support (Fig. 3).

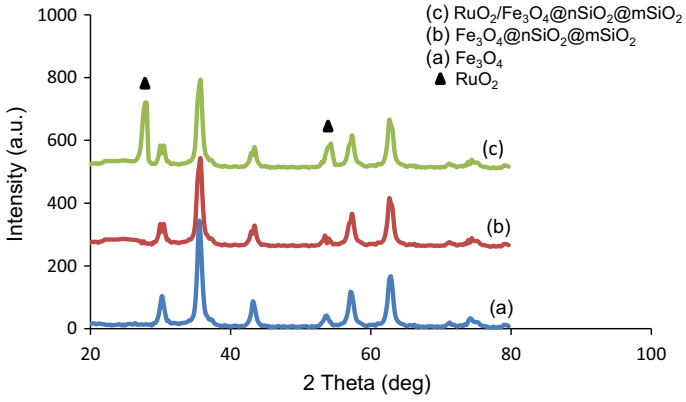

Fig. 1 XRD patterns of Fe_3O_4 (*a*), Fe_3O_4@nSiO_2@mSiO_2 (*b*) and RuO_2/Fe_3O_4@nSiO_2@mSiO_2 (*c*)

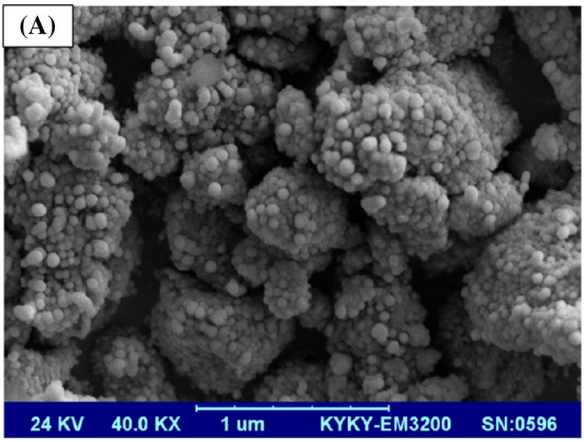
(A)
24 KV 40.0 KX 1 um KYKY-EM3200 SN:0596

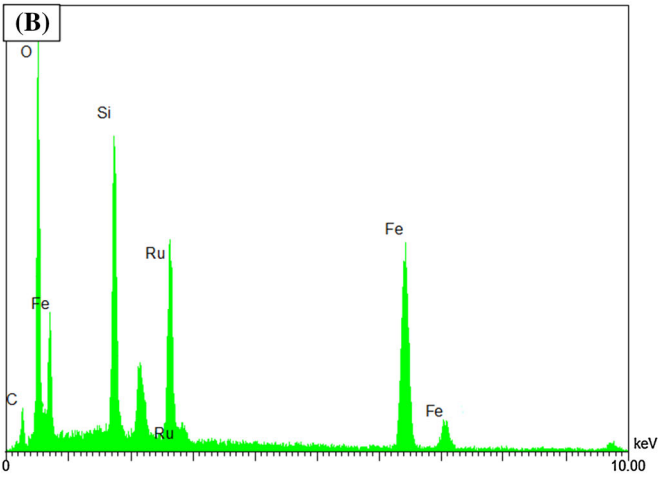
(B)
O
Si
Ru
Fe
Fe
C
Fe
Ru
keV
0
10.00

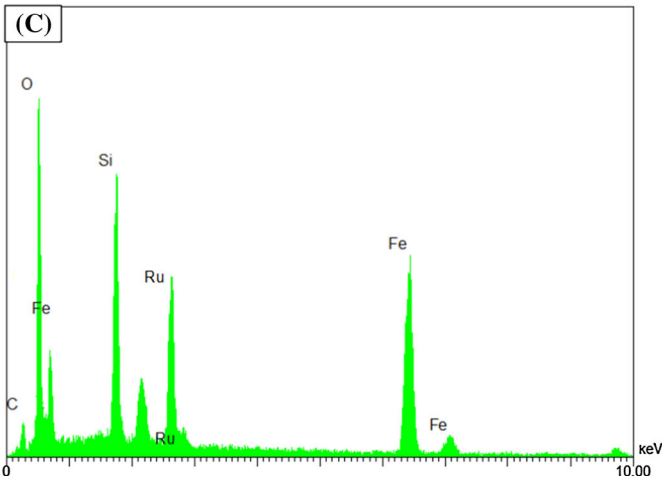
(C)
O
Si
Fe
Ru
Fe
C
Fe
Ru
keV
0
10.00

◀**Fig. 2** SEM image of Fe_3O_4 core nanoparticles (**a**) and EDS spectra of $RuO_2/Fe_3O_4@nSiO_2@mSiO_2$ before reaction (**b**) and after reaction (**c**)

The nitrogen adsorption–desorption isotherms of the support and catalyst samples are displayed in Fig. 4. The specific surface area of $Fe_3O_4@nSiO_2@mSiO_2$ and $RuO_2/Fe_3O_4@nSiO_2@mSiO_2$ were determined to be 394 and 290.8 m^2/g, respectively. This indicates that after RuO_2 loading the specific surface area of the catalyst became lower than the support. The hysteresis loop indicated the mesoporous structure of support and $RuO_2/Fe_3O_4@nSiO_2@mSiO_2$ samples.

Preliminary study of phenol degradation using catalyst

Figure 5 shows preliminary tests of adsorption and phenol degradation in aqueous solution on $Fe_3O_4@nSiO_2@mSiO_2$ and $RuO_2/Fe_3O_4@nSiO_2@mSiO_2$ under various experimental conditions. Generally, $Fe_3O_4@nSiO_2@mSiO_2$ and $RuO_2/Fe_3O_4@nSiO_2@mSiO_2$ are able to adsorb phenol even at low efficiency. Adsorption efficiency can be seen on $Fe_3O_4@nSiO_2@mSiO_2$ and $RuO_2/Fe_3O_4@nSiO_2@mSiO_2$, at 10 % and 4 % in 2 h, respectively. The results indicate that the surface

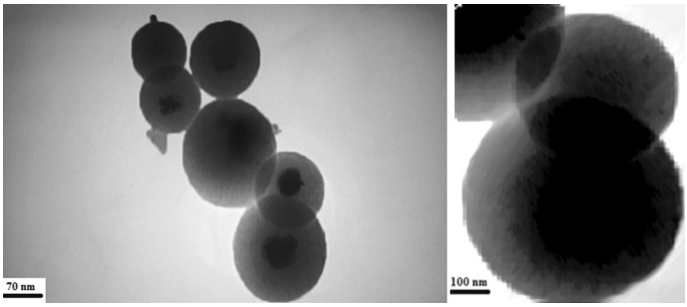

Fig. 3 TEM images of $Fe_3O_4@nSiO_2@mSiO_2$ as support

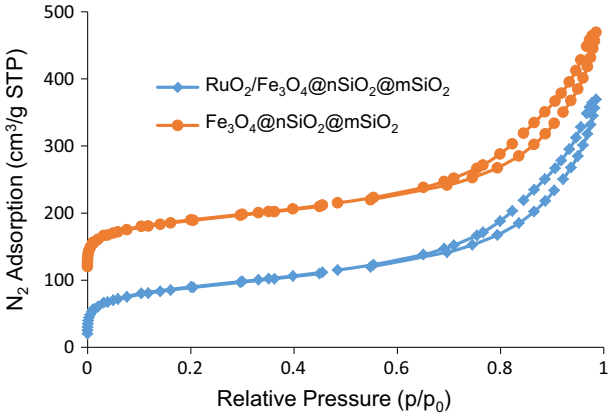

Fig. 4 N_2 adsorption–desorption isotherms of $Fe_3O_4@nSiO_2@mSiO_2$ and $RuO_2/Fe_3O_4@nSiO_2@mSiO_2$

area of support decreases by loading ruthenium on the surface of the Fe_3O_4@-$nSiO_2$@$mSiO_2$. In oxidation experiments, the Oxone without a solid catalyst could not oxidize phenol. Phenol degradation would occur when catalyst and oxidant (PMS) simultaneously were present in the solution. In RuO_2/Fe_3O_4@$nSiO_2$@-$mSiO_2$-Oxone, phenol could be eliminated entirely from solution in 40 min.

Anipsitakis and Dionysiou [29] found that Co (II) and Ru (III) are the best transition metal catalysts for the activation of PMS. The reaction of Ru (III) with PMS can be described as the following:

$$\mathrm{Ru(III)} + \mathrm{HSO_5^-} \rightarrow \mathrm{Ru(IV)} + \mathrm{OH^-} + \mathrm{SO_4^{\cdot -}}. \quad (3)$$

The following procedures show the steps of phenol oxidation:

$$\mathrm{S\text{-}Ru(IV)} + \mathrm{HSO_5^-} \rightarrow \mathrm{S\text{-}Ru(III)} + \mathrm{H^+} + \mathrm{SO_5^{\cdot -}} \quad (\mathrm{S}\text{: solid surface}), \quad (4)$$

$$\mathrm{S\text{-}Ru(III)} + \mathrm{HSO_5^-} \rightarrow \mathrm{S\text{-}Ru(IV)} + \mathrm{OH^-} + \mathrm{SO_4^{\cdot -}}. \quad (5)$$

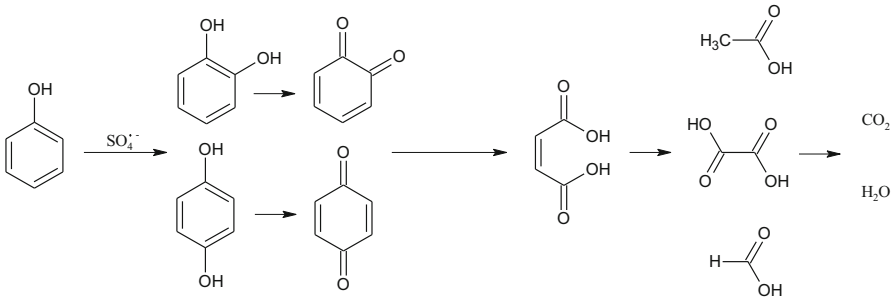

(6)

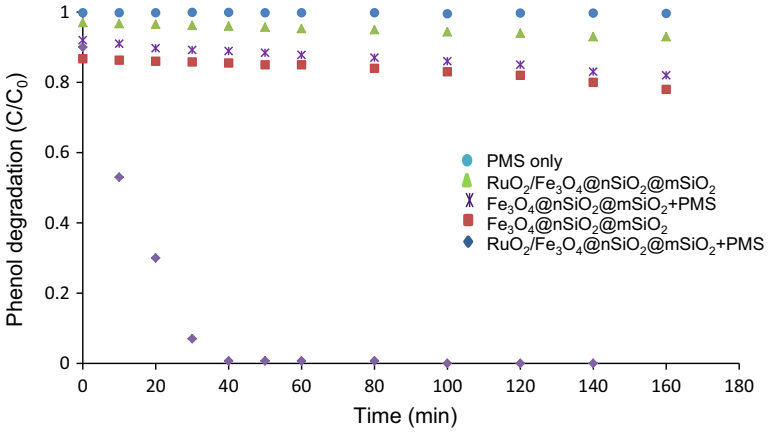

Fig. 5 Phenol removal in various reaction conditions

At first, catechol was produced in the presence of sulfate radicals and then converted to hydroquinone and benzoquinone [30–32]. Maleic acid, oxalic acid, and acetic acid, as the latter intermediates, were finally mineralized to CO_2 and H_2O [33].

Figure 6 shows photographs of $RuO_2/Fe_3O_4@nSiO_2@mSiO_2$ dispersion in phenol solution at ambient temperature and the magnetic separation process. As illustrated in the photograph, the suspension is stable and homogeneous before magnetic separation. In the presence of a magnet, the particles in the suspension can be separated fast and accumulated on the side wall of the glass vial near the magnet. After removing the magnet, particles were rapidly redispersed in solution. This indicates that the sample possessed good water dispersion and magnetic separation.

Effects of reaction parameters on phenol degradation

Figure 7 shows various concentrations of phenol (between 20 and 100 ppm) on the phenol degradation. At low phenol concentrations (20-50 ppm), 100 % phenol degradation could be achieved within 40 min. At a phenol concentration of 100 ppm, degradation efficiency was only 55 % within 2 h.

Degradation of phenol in the solution depends on the amount of the $RuO_2/Fe_3O_4@nSiO_2@mSiO_2$ catalyst (Fig. 8). Phenol oxidation efficiency is enhanced by increasing catalyst dosage in the solution. At 0.1 g $RuO_2/Fe_3O_4@nSiO_2@mSiO_2$, phenol degradation would be 88 % at 80 min, while with $RuO_2/Fe_3O_4@nSiO_2@mSiO_2$ loading of 0.2 g, oxidation of phenol would reach 100 % at 40 min.

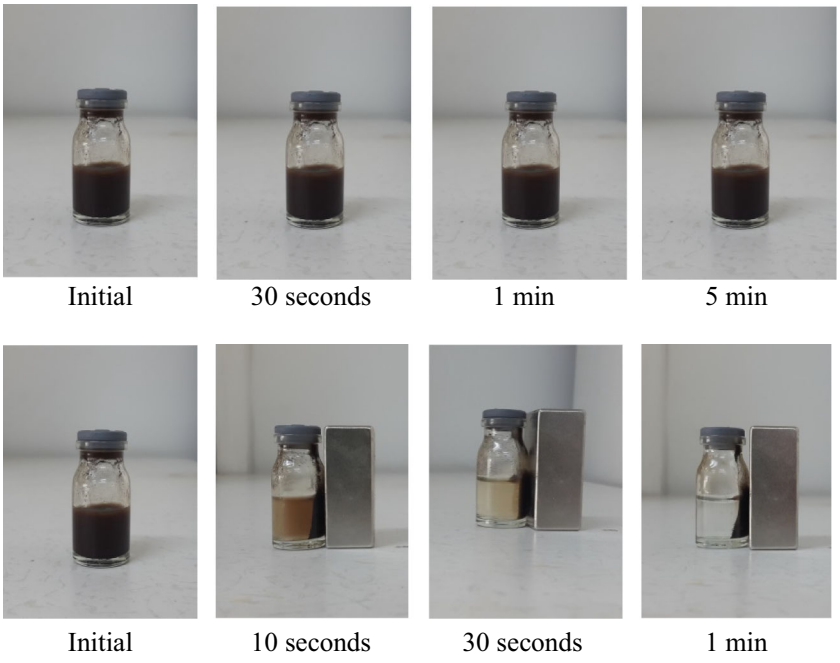

Fig. 6 Photos of magnetic separation of $RuO_2/Fe_3O_4@nSiO_2@mSiO_2$

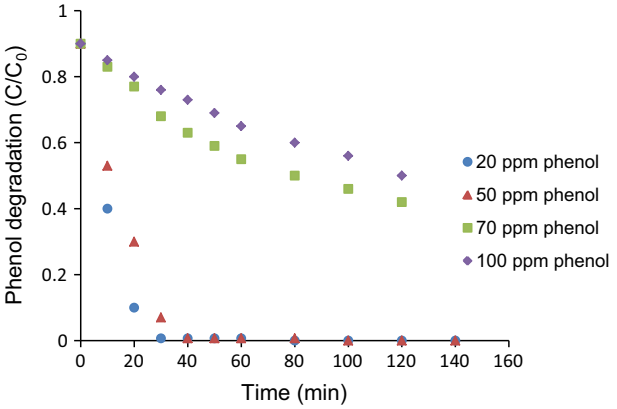

Fig. 7 Effect of phenol concentration on phenol removal. $RuO_2/Fe_3O_4@nSiO_2@mSiO_2$. Reaction conditions: 1 g Oxone, 0.2 g catalyst, 25 °C

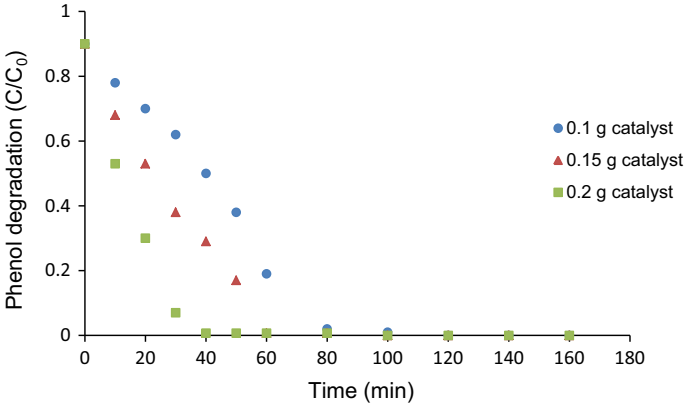

Fig. 8 Effect of catalyst loading on phenol removal. $RuO_2/Fe_3O_4@nSiO_2@mSiO_2$. Reaction conditions: 50 ppm, 1 g Oxone, 25 °C

Figure 9 shows that degradation of phenol depends on the concentration of Oxone. At 0.2 g Oxone, 85 % removal of phenol could be achieved in about 80 min. When the concentration of oxidant component was increased to 1 g, phenol could be fully removed within 40 min. Degradation efficiency would decrease at extra Oxone loading. It has been reported that the self-quenching phenomenon of hydroxyl and sulfate ions by PMS is possible as shown below [34]:

$$OH^{\cdot} + HSO_5^- \rightarrow H_2O + SO_5^{\cdot -}, \quad (7)$$

$$SO_4^{\cdot -} + HSO_5^- \rightarrow H^+ + SO_5^{\cdot -}. \quad (8)$$

Extra amounts of HSO_5^- from Oxone would consume the active $SO_4^{\cdot -}$.

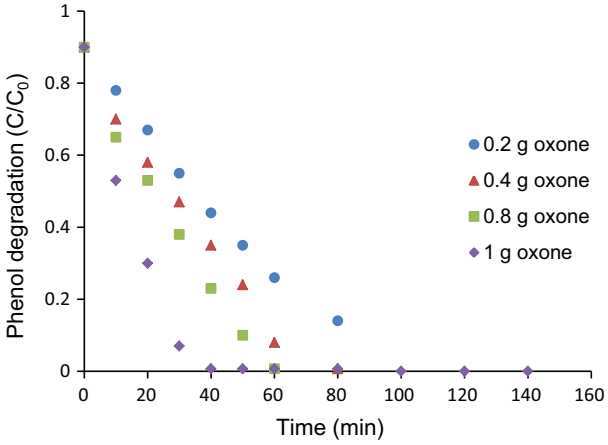

Fig. 9 Effect of Oxone concentration on phenol removal. $RuO_2/Fe_3O_4@nSiO_2@mSiO_2$. Reaction conditions: 50 ppm, 0.2 g catalyst, 25 °C

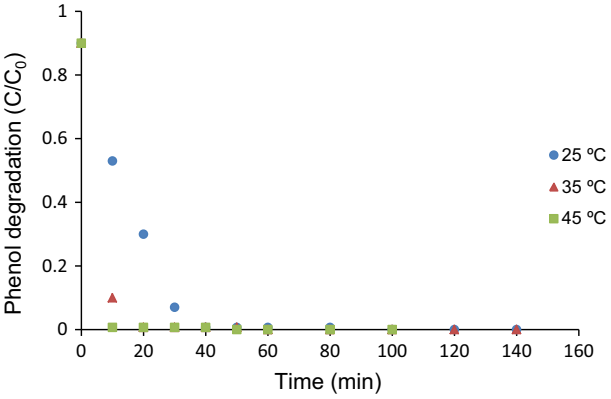

Fig. 10 Effect of temperature on phenol removal. $RuO_2/Fe_3O_4@nSiO_2@mSiO_2$. Reaction conditions: 50 ppm, 1 g Oxone, 0.2 g catalyst

The effect of reaction temperature on phenol degradation is shown in Fig. 10. As can be seen, the rate of reaction would increase considerably with increase in temperature. Complete phenol degradation at a temperature of 25 °C could be achieved in 40 min. When the temperature was raised to 35 °C, 100 % degradation efficiency of phenol could be achieved in about 20 min. At 45 °C complete removal could be achieved in about 10 min.

The catalyst was used once before the regeneration process, and then it was tested after its regeneration by annealing in air, using ultrasonication, and washing with water. The deactivation of catalyst occurs probably due to adsorption of intermediates and a fraction of loose ruthenium leaching from the support. A 100 % phenol removal was achieved after 50 min for the catalyst regenerated by

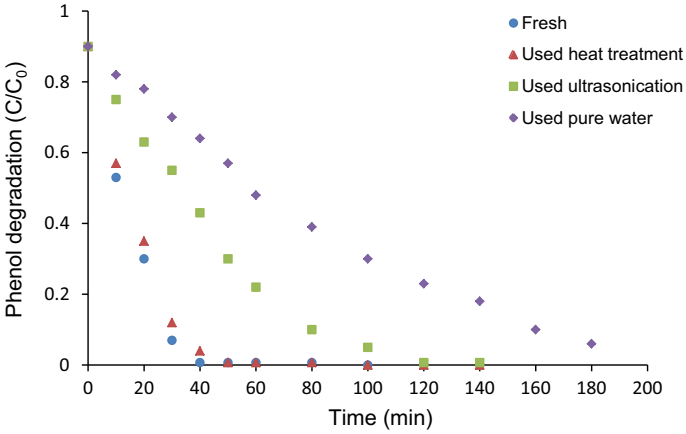

Fig. 11 Regeneration studies of the used catalyst

annealing in air. This shows that the catalytic activity of the catalyst was recovered thoroughly by heat treatment and surface-attached intermediates were removed, whereas regeneration of the used catalyst by applying ultrasonic and washing with water partially eliminated the intermediates present on the surface of the catalysts (Fig. 11).

Conclusions

In this study, Fe_3O_4/silica spheres have been synthesized by hydrolysis reaction and ruthenium oxide loaded on the support was prepared by an impregnation method. $RuO_2/Fe_3O_4@nSiO_2@mSiO_2$ is an effective catalyst for heterogeneous activation of PMS for phenol degradation. Parameters such as the amount of catalyst, temperature, and phenol and PMS concentration have important roles in phenol oxidation. The catalyst was tested after its regeneration by annealing in air, using ultrasonication, and washing with water. Regeneration by annealing in air could recover the catalyst activity completely.

References

1. V. Dohnal, D. Fenclova, J. Chem. Eng. Data **40**, 478 (1995)
2. M. Anbia, S. Amirmahmoodi, Scientia Iranica **18**, 446 (2011)
3. M. Anbia, A. Ghaffari, Appl. Surf. Sci. **255**, 9487 (2009)
4. J. Dona, C. Garriga, J. Arana, J. Pérez, G. Colon, M. Macías, J. Navio, Res. Chem. Intermed. **33**, 351 (2007)
5. Y. Yang, C. Tian, Res. Chem. Intermed. **38**, 583 (2012)
6. A. Fortuny, C. Bengoa, J. Font, A. Fabregat, J. Hazard. Mater. **64**, 181 (1999)
7. S.G. Christoskova, M. Stoyanova, M. Georgieva, Appl. Catal. A-Gen. **208**, 243 (2001)

8. P.R. Shukla, S. Wang, H. Sun, H.M. Ang, M. Tadé, Appl. Catal. B-Environ. **100**, 529 (2010)
9. J. Barrault, M. Abdellaoui, C. Bouchoule, A. Majeste, J. Tatibouet, A. Louloudi, N. Papayannakos, N. Gangas, Appl. Catal. B-Environ. **27**, 225 (2000)
10. C.-P. Huang, Y.-H. Huang, Appl. Catal. A-Gen. **346**, 140 (2008)
11. S. Chiron, A. Fernandez-Alba, A. Rodriguez, E. Garcia-Calvo, Water Res. **34**, 366 (2000)
12. A. Garg, I.M. Mishra, S. Chand, Clean-Soil Air Water **38**, 27 (2010)
13. J. Zazo, J. Casas, A. Mohedano, M. Gilarranz, J. Rodriguez, Environ. Sci. Technol. **39**, 9295 (2005)
14. S. Imamura, A. Hirano, N. Kawabata, Ind. Eng. Chem. Prod. Dev. **21**, 570 (1982)
15. S. Wang, Dyes Pigments **76**, 714 (2008)
16. P. Gallezot, S. Chaumet, A. Perrard, P. Isnard, J. Catal. **168**, 104 (1997)
17. S. Imamura, A. Doi, S. Ishida, Ind. Eng. Chem. Prod. Dev. **24**, 75 (1985)
18. S. Esplugas, J. Gimenez, S. Contreras, E. Pascual, M. Rodríguez, Water Res. **36**, 1034 (2002)
19. G.P. Anipsitakis, D.D. Dionysiou, Environ. Sci. Technol. **37**, 4790 (2003)
20. G.P. Anipsitakis, D.D. Dionysiou, Appl. Catal. B-Environ. **54**, 155 (2004)
21. K. Pirkanniemi, M. Sillanpää, Chemosphere **48**, 1047 (2002)
22. L. Oliviero, J. Barbier, D. Duprez, A. Guerrero-Ruiz, B. Bachiller-Baeza, I. Rodrıguez-Ramos, Appl. Catal. B-Environ. **25**, 267 (2000)
23. M. Carrier, M. Besson, C. Guillard, E. Gonze, Appl. Catal. B-Environ. **91**, 275 (2009)
24. W.-M. Liu, Y.-Q. Hu, S.-T. Tu, J. Hazard. Mater. **179**, 545 (2010)
25. D.P. Minh, P. Gallezot, M. Besson, Appl. Catal. B-Environ. **63**, 68 (2006)
26. H. Wang, H. Tian, Z. Hao, J. Environ. Sci. **24**, 536 (2012)
27. Y. Kang, L. Zhou, X. Li, J. Yuan, J. Mater. Chem. **21**, 3704 (2011)
28. S. Gai, P. Yang, C. Li, W. Wang, Y. Dai, N. Niu, J. Lin, Adv. Funct. Mater. **20**, 1166 (2010)
29. G.P. Anipsitakis, D.D. Dionysiou, Environ. Sci. Technol. **38**, 3705 (2004)
30. G.P. Anipsitakis, D.D. Dionysiou, M.A. Gonzalez, Environ. Sci. Technol. **40**, 1000 (2006)
31. F. Mijangos, F. Varona, N. Villota, Environ. Sci. Technol. **40**, 5538 (2006)
32. M.S. Yalfani, S. Contreras, F. Medina, J. Sueiras, Appl. Catal. B-Environ. **89**, 519 (2009)
33. L. Hu, X. Yang, S. Dang, Appl. Catal. B-Environ. **102**, 19 (2011)
34. P. Shukla, I. Fatimah, S. Wang, H. Ang, M.O. Tadé, Catal. Today **157**, 410 (2010)